Analytical and Bioanalytical Chemistry
https://doi.org/10.1007/s00216-022-04380-1

RESEARCH PAPER

CRISPR/Cas13a combined with hybridization chain reaction for visual detection of influenza A (H1N1) virus

Hongyu Zhou[1,2] · Shengjun Bu[2] · Yao Xu[2] · Lulu Xue[2] · Zhongyi Li[2] · Zhuo Hao[2] · Jiayu Wan[2] · Feng Tang[1]

Received: 8 August 2022 / Revised: 21 September 2022 / Accepted: 11 October 2022

Abstract

This study provides proof of concept of a colorimetric biosensor for influenza H1N1 virus assay based on the CRISPR/Cas13a system and hybridization chain reaction (HCR). Target RNA of influenza H1N1 virus activated the trans-cleavage activity of Cas13a, which cleaved the special RNA sequence (-UUU-) of the probe, further initiating HCR to copiously generate G-rich DNA. Abundant G-quadruplex/hemin was formed in the presence of hemin, thus catalyzing a colorimetric reaction. The colorimetric biosensor exhibited a linear relationship from 10 pM to 100 nM. The detection limit was 0.152 pM. The biosensor specificity was excellent. This new and sensitive detection method for influenza virus is a promising rapid influenza diagnostic test.

Keywords Influenza H1N1 virus detection · CRISPR/Cas13a · Hybridization chain reaction · DNAzyme

Introduction

Influenza virus is an enveloped, segmented, negative-stranded, single-stranded RNA virus [1]. Most warm-blooded animals can become the host of influenza virus. Influenza virus is a serious threat to human health and has historically caused many pandemics, with considerable morbidity and mortality worldwide [2]. Currently, influenza viruses comprise types A, B, C, and D [3, 4]. Influenza A virus is the most severe and deadly. Among them, influenza A (H1N1) virus (hereafter influenza H1N1), which has three different RNA fragment sequences, can be isolated from swine, avian, and humans [5]. In one year, this virus spread to 214 countries, causing more than 18,000 deaths worldwide, and has become a major international public health problem [6]. Developing a sensitive, specific, rapid, and reliable sensor of H1N1 is essential for controlling outbreaks.

Virus isolation and culture was the gold standard for diagnosing influenza virus. This has been supplanted by reverse transcriptase polymerase chain reaction (RT-PCR), with its superior analytical and clinical sensitivity [7]. Concurrently, several traditional detection methods are widely used in the detection of influenza virus. These include ELISA [8] and protein identification [9]. The traditional detection of influenza viruses has improved with time. However, the method has some inherent disadvantages. It is complicated to perform and require professionally trained personnel or sophisticated laboratory instruments. Therefore, this technique is not suitable for routine healthcare and resource-poor areas [10]. Many alternative methods have been assessed for the detection of influenza viruses. These include an electrochemical immunosensor [11], a surface-enhanced Raman scattering–based imaging aptasensor platform [12], fluorescence [13], colorimetric [14], immunochromatographic [15], and microfluidic chip [16] approaches. Among them, colorimetry is a fast and convenient option that does not require advanced instruments.

Despite promising progress in emerging diagnostic tests to detect influenza virus, a perfect detection method has yet to be developed. Clustered regularly interspaced short palindromic repeats (CRISPR)/Cas systems have attracted a lot of attention due to their simplicity. Only one single effector is required. The CRISPR-Cas module present in most archaea and many bacteria belongs to the adaptive immune system

✉ Jiayu Wan
wanjiayu@hotmail.com

✉ Feng Tang
tangfeng@jzmu.edu.cn

[1] College of Animal Husbandry and Veterinary Medicine, Jinzhou Medical University, Jinzhou 121001, China

[2] Changchun Veterinary Research Institute, Chinese Academy of Agricultural Sciences, Changchun 130122, China

Published online: 20 October 2022

and provides sequence-specific protection to RNA in the presence of foreign invading DNA [17]. The CRISPR family is used for gene editing and transcriptional regulation [18], and is also widely used in biosensing. Examples of the latter include detection of DNA [19] and microRNA [20]. Cas13a was first proposed in 2016 [21]. Compared with the other Cas proteins (Cas9, Cas12a, Cas14), Cas13 can directly detect RNA without reverse transcription because Cas13a is a single-stranded (ss) RNA-targeted RNase that exhibits both cis- and trans-cleavage activities [22]. In particular, Cas13a can directly and specifically recognize target RNA and subsequently activate its trans-cleavage activity. The resulting nonspecific cleavage of nearby RNAs makes Cas13a more suitable for detection of RNA than other Cas proteins. Cas13a is used in a variety of RNA detection methods, such as microRNA [23], SARS-CoV-2 [24], and RNA N6-methyl-adenosine [25].

To further improve analysis performance, the Cas13a system has been combined with various signal amplification techniques, such as rolling circle amplification (RCA) [26], recombinase polymerase amplification (RPA) [27], and loop-mediated isothermal amplification (LAMP) [28]. Some of these isothermal nucleic acid amplification techniques employ expensive enzymes, some are tedious to perform since they require reverse transcription, and the correct design of species-specific primers is challenging for some. Toehold-mediated strand displacement reactions have received extensive attention due to their superior cascade properties in terms of cost, programmability, universality, and modularity [29]. Hybridization chain reaction (HCR) is a toehold-mediated strand displacement reaction first developed by Dirks and Pierce [30]. HCR is an enzyme-free, entropy-driven, isothermal spontaneous DNA assembly process [31]. An ordinary HCR needs three components including one DNA initiator and two DNA hairpins, In particular, two stable DNA hairpins coexist in solution until the first hairpin is opened after a promoter strand is introduced. The loss of secondary structure leads to the opening of a second and similar hairpin. This process is a series of DNA assembly events. Ultimately, the HCR forms a nicked double helix with many repeating units. Compared with PCR, HCR is used for isothermal nucleic acid amplification without cumbersome temperature changes. Compared with RCA and LAMP, HCR does not require enzymes and a complex primer design, respectively.

Here, we introduce horseradish peroxidase–mimicking DNAzyme (HRP-DNAzyme) to combine Cas13a and HCR. HRP-DNAzyme is one of the most commonly used catalytic DNAzymes in biosensors and biorecognition. The single-stranded guanine-rich nucleic acid and hemin complex components [32] interact to catalyze a redox reaction between hydrogen peroxide (H_2O_2) and 2,2′-azino-bis(3-ethyl-benzothiozoline)-6-sulfonic acid ($ABTS^{2-}$) with an accompanying color change [33]. This method does not require cumbersome instruments and expensive modified probes (such as fluorophores, quenchers, methylene blue, etc.) to achieve the transduction of analyte recognition events into an optical detection mode. The colorimetric biosensor amplifies the signal and reduces the experimental conditions to visually detect influenza H1N1. We observed an excellent linear relationship of the colorimetric biosensor from 10 pM to 100 nM, with a detection limit of 0.152 pM. Because of the outstanding selectivity of Cas13a, unexpected influenza A virus subtypes can be excluded in the amplification reaction. The data presented here demonstrate that this Cas13a-based colorimetric biosensor is a promising analytical method for biological analyses and clinical diagnoses.

Experimental section

Reagents and instruments

All DNA sequences used in this study were synthesized by Sangon Biotechnology Co., Ltd. (Shanghai, China). All the oligonucleotides are given in Table S1 (see Supplementary information Table S1). The HiScribe T7 High Yield RNA Synthesis Kit and Monarch RNA Purification Columns were obtained from New England BioLabs (Ipswich, MA, USA). Trizol Reagent and Dynabeads M-270 Streptavidin (magnetic beads [MBs], 2.8 μm in diameter, 10 mg/mL) were provided by Thermo Fisher Scientific (Waltham, MA, USA). Purified *Leptotrichia wade* (Lwa)Cas13a protein and LwaCas13a buffer were obtained from Tolo Biotech (Shanghai, China). RNase inhibitor was obtained from Promega Corporation (Madison, WI, USA). Hemin and AzBTS-$(NH_4)_2$ were purchased from Sigma-Aldrich, Inc. (Saint Louis, MO, USA). RNase-free water and all chemicals were bought from Sangon Biotechnology (Shanghai, China) and used without further purification. The allantoic fluid of chick embryos infected with influenza H1N1 was stored and provided by Changchun Veterinary Research Institute, Chinese Academy of Agricultural Sciences. Absorbance measurements were measured using a Nano Drop ND-1000 spectrophotometer (Thermo Fisher Scientific).

Preparation of crispr (cr)RNA and target RNA by in vitro transcription

The target RNA sequence was designed according to the specific sequence fragment of influenza H1N1. Mature LwaCas13a crRNA was designed. It contained a 36-nucleotide (nt) direct repeat sequence and a 25-nt spacer that was completely complementary to the target RNA. The crRNA and target RNA were synthesized by in vitro transcription using T7 RNA polymerase and the HiScribe T7 High Yield

RNA Synthesis Kit (New England Biolabs) to transcribe and Monarch RNA Cleanup Kit to purify RNA. Two microliters of 100 μM T7 promoter, 2 μL of 100 μM ssDNA templates containing T7 promoter sequence, and 14 μL RNase-free water were incubated at 95 °C for 5 min and then gradient cooled to 25 °C. The transcription reaction was established with the above solution, 2 μL T7 RNA polymerase (50 U/μL), and 10 μL NTP Buffer mix (20 mM) at 37 °C for 16 h. Then, 2 μL DNaseI (2 U/μL) was added and mixed to degrade the DNA in the solution. The concentrations of crRNA and target RNA were determined using a Nanodrop 1000 UV–vis spectrophotometer (Thermo Fisher Scientific) and stored at – 80 °C.

Detection of influenza H1N1

Ten microliters of a CRISPR/Cas13a cleavage reaction system contained 1 μL of various concentrations of target ssRNA, 1 μL of 0.5 μM crRNA, 1 μL of 5 U RNase inhibitor, 1 μL of 0.8 μM Cas13a protein, 2 μL of 1 × Cas13a buffer, and 4 μL of 1.25 μM probe I. The mixture was incubated at 37 °C for 30 min, followed by deactivation of Cas13a enzyme activity at 80 °C for 10 min. Streptavidin-coated MBs (SA-MBs) were prepared according to standard methods. Five microliters of a suspension of SA-MBs (10 mg/mL) was rinsed three times with 15 μL of PBS buffer (0.08 mM NaH_2PO_4 and 0.02 mM Na_2HPO_4, pH 7.4). The SA-MBs were resuspended in 5 μL Tris–HCl buffer (20 mM Tris, 2 mM $MgCl_2$, 200 mM NaCl, 20 mM KCl, pH 7.4). The obtained Cas13a cleavage product was added to the suspension of SA-MBs, and the mixture was incubated at 37 °C for 10 min. Subsequently, the beads were separated using a magnet and the supernatant was transferred to a new centrifuge tube. Ten microliters of 2 μM H1 and 10 μL of 1.5 μM H2 were added to the solution followed by heating at 37 °C for 40 min. Ten microliters of 10 μM hemin was added and reacted at 37 °C for 40 min. Finally, 10 μL of 50 mM ABTS was added, followed by 10 μL of 40 mM H_2O_2. The solution was incubated at room temperature for 5 min. The absorbance of the resulting samples at a wavelength of 414 nm was measured by a Nano Drop ND-1000 spectrophotometer.

Native polyacrylamide gel electrophoresis (PAGE) analysis

The products of Cas13a/crRNA trans-cleavage and HCR were analyzed using 15% native PAGE. Ten microliters of product and 2 μL of 6 × loading buffer were mixed evenly. Ten microliters of mixed liquid was loaded in the gel lane. The gel was run in 1 × TBE (89 mM Tris, 89 mM boric acid, 2.0 mM EDTA, pH 8.2) at 180 V for 40 min. The gel was dyed by SYBR Green I for 15 min and imaged using a C600 ultimate western blot imaging system (Azure Biosystems, Dublin, CA, USA).

Extraction of total viral RNA from chicken embryo allantoid fluid

The allantoic fluid of chick embryos infected with influenza H1N1 was collected. The total viral RNA was extracted by Trizol method. Two hundred fifty microliters of sample was thoroughly mixed with 750 μL of Trizol reagent and allowed to stand for 10 min at room temperature. Two hundred microliters of chloroform was added and mixed by violent oscillation for 30 s and allowed to stand for 10 min at room temperature. The solution was centrifuged at 12,000 rpm for 15 min at 4 °C. At this time, the solution appeared layered. Five hundred microliters of the supernatant was transferred to a new enzyme-free tube. Five hundred microliters of isopropanol was added; the contents were gently inverted several times to mix and allowed to stand for 10 min at room temperature. After centrifugation at 12,000 rpm for 10 min at 4 °C, the supernatant was discarded, and the pellet was resuspended in 750 μL of cold 75% ethanol. The mixture was centrifuged at 12,000 rpm for 5 min at 4 °C. The supernatant was also discarded. Finally, the total viral RNA was resuspended in 50 μL RNase-free water and stored at – 80 °C.

Results and discussion

Principle of H1N1 influenza detection

Here, we developed a dual signal amplification strategy based on Cas13a for a visual assay of influenza H1N1. In the principle depicted in Scheme 1, the first step is the recognition of H1N1 by the colorimetric biosensor and ensured specificity of the reaction by the CRISPR/Cas13a protein system. Target RNA extracted from influenza H1N1 is bound to crRNA through base complementation pairing after entering the interior of the CRISPR/Cas13a protein. This alters the protein structure and activates the trans-cleavage ability of the CRISPR/Cas13a protein. A DNA oligonucleotide strand containing three uridine monophosphate was created (probe I). The probe was designed to serve as the substrate for trans-cleavage of Cas13a/crRNA. DNA probe I consists of an I_1 strand at the 5′ end, a special RNA sequence (-UUU-) in the middle, and an I_2 strand at the 3′ end. Modification of the I_1 strand with biotin allows the strand to initiate the HCR. The special RNA sequence (-UUU-) is recognized and cut by the CRISPR/Cas13a system. Cas13a is activated and cleaves the RNA sequence of probe I, which separates the I_1 and I_2 strands. The SA-MBs are added, and the biotin interacts with SA. The uncleaved probe I and I_1 strands containing biotin are adsorbed by the SA-MBs, which are

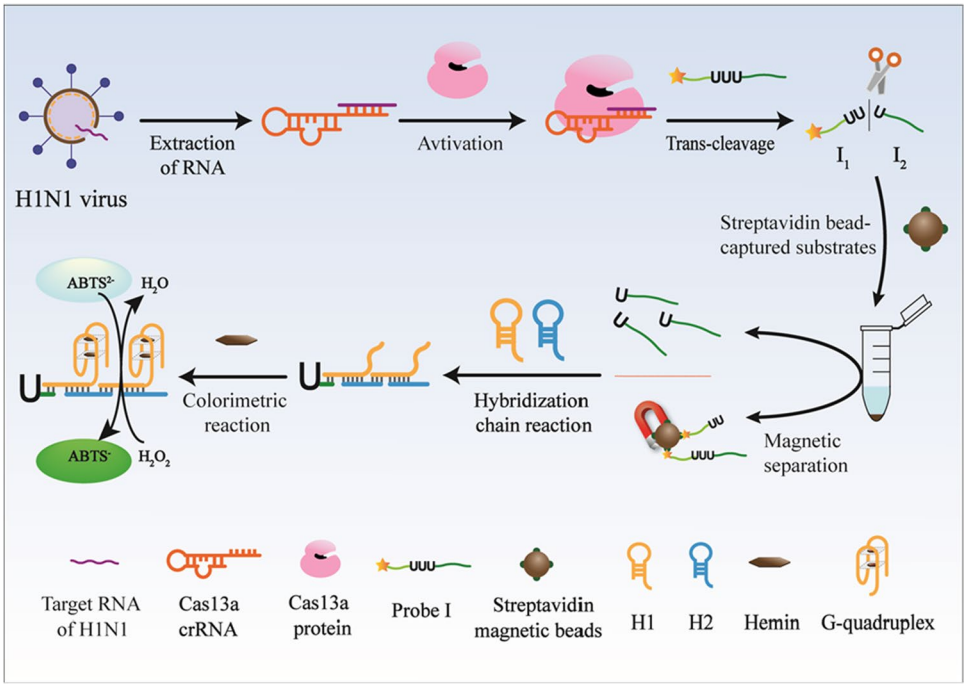

Scheme 1 Schematic illustration of CRISPR/Cas13a combined with hybridization chain reaction for visual detection of influenza H1N1

then removed from the solution by magnetic separation. After adding hairpin DNA H1 and H2, the I_2 chain conjugates with H1 and opens the H1 hairpin via toehold-mediated strand displacement. Hybridization of the I_2-H1 complex opens the hairpin structure of H2. The opened H2 chain is complementary to the hairpin H1 chain, which results in the opening of the hairpin structure of the H1 strand, thereby initiating the HCR. Because the H1 and H2 hairpin structures are continuously opened and assembled, the G-quadruplex fragment of H1 is exposed. Subsequently, in the presence of hemin, the G-quadruplex structure folds and hemin intercalates into the structure to form a DNAzyme. The G-quadruplex DNAzyme can catalyze the redox reaction between $ABTS^{2-}$ and H_2O_2. The color of the ABTS solution changes from light green to dark green. The resulting colorimetric reaction produces a color change of the reaction solution that is visible to the naked eye, permitting the ultra-sensitive visual detection of influenza H1N1.

Experimental feasibility analysis

To verify the feasibility of the CRISPR/Cas13a cleavage effect, the CRISPR/Cas13a cleaved product was examined by PAGE. Lanes 1–3 of Fig. 1A respectively contain bands without Cas13a, without crRNA, and without target RNA in the complete Cas13a/crRNA trans-cleavage system. Lane 4 contains the complete system. In contrast to lane 4, lanes 1–3 displayed a pronounced band at the same location. Conversely, the band of lane 4 at this location was weaker, with the appearance of new bands of cleaved probe I further down in the gel. Only in the complete system was the target RNA of influenza H1N1 able to activate the Cas13a/crRNA trans-cleavage system. In addition, the trans-cleavage ability of Cas13a was confirmed by PAGE again. As shown in Supplementary information Figure S1, a low concentration of H1N1 could activate the CRISPR/Cas13a system to cleave a high concentration of probe I, and in this range, probe I could be completely cleaved.

Subsequently, the activated Cas13a/crRNA trans-cleavage system cleaved the DNA probe I to produce the I_1 and I_2 chains. The feasibility of the detection system was verified by PAGE. The I_2 strand commenced the subsequent HCR to generate H1–H2 double helices (Fig. 1B). Lanes 1 and 2 show that H1 and H2 were both in monomeric form. Lane 3 displays the situation when H1 and H2 coexist. Lane 4 shows a nicked double-helix structure formed when DNA probes I, H1, and H2 coexist. Lane 5 and 6 display the co-mixture of H1 and H2 after adding the Cas13a/crRNA system and MBs in the absence (lane 5) and presence (lane 6) of H1N1 target RNA. As anticipated, high molecular weight bands with extremely low electrophoretic mobility were generated in lanes 4 and 6. In contrast, these bands were absent in lanes 3 and 5. Compared to lanes 1 and 2, the H1 and H2 bands were less prominent in lanes 4 and 6, and were absent in lanes 3 and 5. The findings demonstrate the successful initiation of HCR and verifies the separation capability of the MBs for further development of the colorimetric biosensor.

G-quadruplex formation, catalysis, and the overall feasibility of the protocol were validated using colorimetry. The products in each of the above lanes were incubated with hemin, followed by the addition of hemin and $ABTS^{2-}$. As

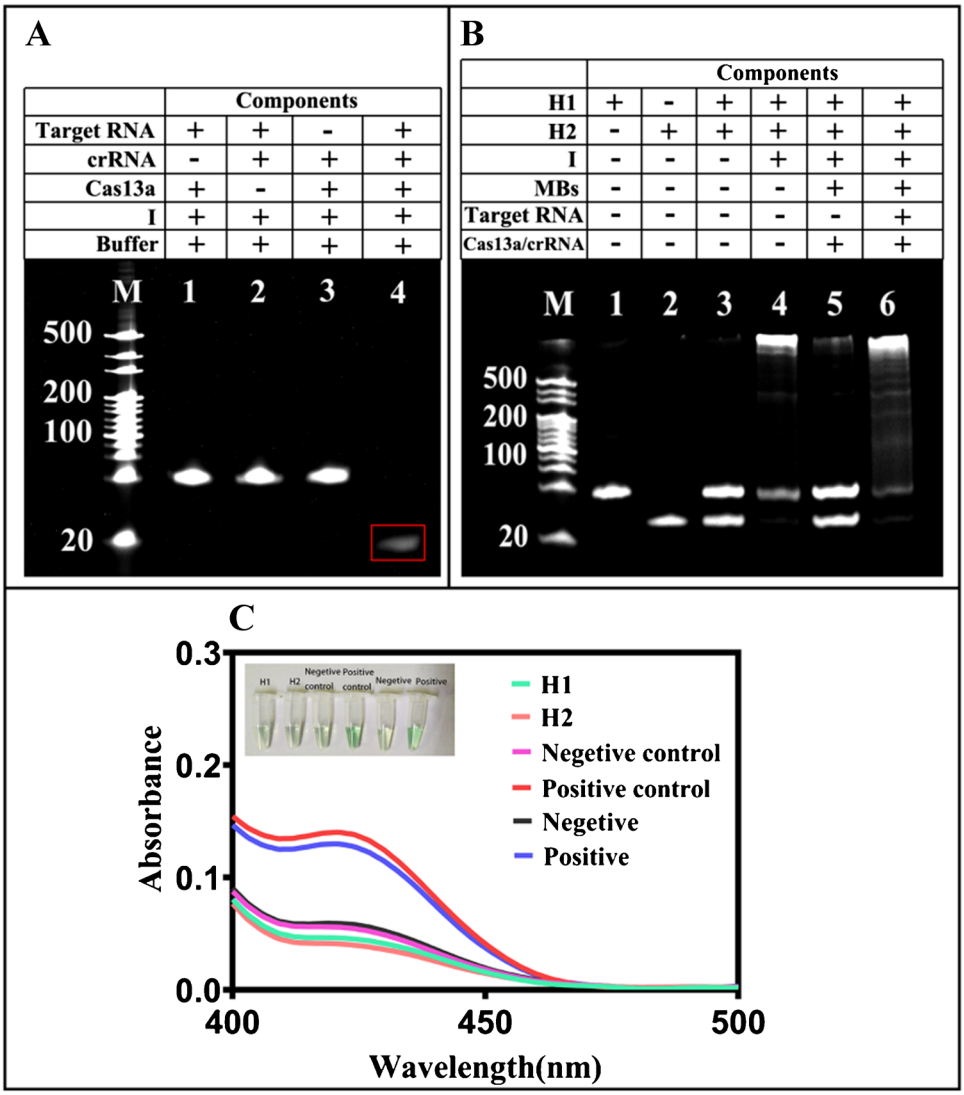

Fig. 1 **A** Nondenaturing 15% PAGE analysis of cleavage ability of Cas13a for probe I. M: 20 bp DNA ladder. Lane 1: 1 μM target RNA, 0.8 μM Cas13a, 1.25 μM I. Lane 2: 1 μM target RNA, 0.5 μM crRNA, 1.25 μM I. Lane 3: 0.5 μM crRNA, 0.8 μM Cas13a, 1.25 μM I. Lane 4: 1 μM target RNA, 0.5 μM crRNA, 0.8 μM Cas13a, 1.25 μM I. **B** Nondenaturing 15% PAGE analysis of the ability of magnetic beads (MBs) and the result of HCR. M: 20 bp DNA ladder. Lane 1: 2 μM H1. Lane 2: 1.5 μM H2. Lane 3: 2 μM H1, 1.5 μM H2. Lane 4: 1.25 μM I, 2 μM H1, 1.5 μM H2. Lane 5: 2 μM H1, 1.5 μM H2, 1.25 μM I, 10 μg MBs, 0.5 μM crRNA, 0.8 μM Cas13a. Lane 6: 2 μM H1, 1.5 μM H2, 1.25 μM I, 10 μg MBs, 1 μM target RNA, 0.5 μM crRNA, 0.8 μM Cas13a. **C** Feasibility analysis of the formation and catalysis of G-quadruplex. Negative control: 2 μM H1, 1.5 μM H2. Positive control: 1.25 μM I, 2 μM H1, 1.5 μM H2. Negative: 2 μM H1, 1.5 μM H2, 1.25 μM I, 10 μg MBs, 0.5 μM crRNA, 0.8 μM Cas13a. Positive: 2 μM H1, 1.5 μM H2, 1.25 μM I, 10 μg MBs, 1 μM target RNA, 0.5 μM crRNA, 0.8 μM Cas13a

shown in Fig. 1C, in positive samples and positive control samples, the colorless mixture turned green. Only these samples displayed a significant increase in absorption intensity. The absorbance of the positive sample was almost indistinguishable from that of the positive control sample.

Optimization of experimental conditions

To maximize the detection of influenza H1N1 viruses, pivotal assay factors that needed to be optimized were the concentration of Cas13a, CRISPR/Cas13a cleavage temperature, the concentration ratio of Na^+ to K^+, the concentration of probe I, the concentration ratio of hairpin H1 and H2, the concentration of hemin solution, CRISPR/Cas13a cleavage time, and HCR time. The ratio of I/I_0, in which I is the absorbance in the presence of the target RNA and I_0 is the absorbance in the absence of target RNA, was used to evaluate the performance of the assay parameters.

The concentration of Cas13a/crRNA affected the degree of the trans-cleavage of probe I, which influenced the amplification efficiency of subsequent HCRs. As shown in Fig. 2A, the I/I_0 value varied with the concentration of Cas13a/crRNA and tended to be stable when the concentration of Cas13a/crRNA was ≥ 0.8 μM. This concentration was determined to be the optimum concentration of Cas13a/crRNA. The I/I_0 value changed with the difference Cas13a/crRNA trans-cleavage temperature (Fig. 2B). When the temperature was 37 ℃, the value of I/I_0 was maximum. When the temperature value exceeded 37 ℃, there was a subsequent decrease in the value of I/I_0. The findings indicated that a temperature that was too high would affect the activity of the Cas13a protein. Insufficient probe I was not conducive to HCRs, while excess probe I increased the background signal. The I/I_0 value gradually increased from 0.25 to 1.75 μM with increasing probe I concentration (Fig. 2C). When the concentration of probe I exceeded

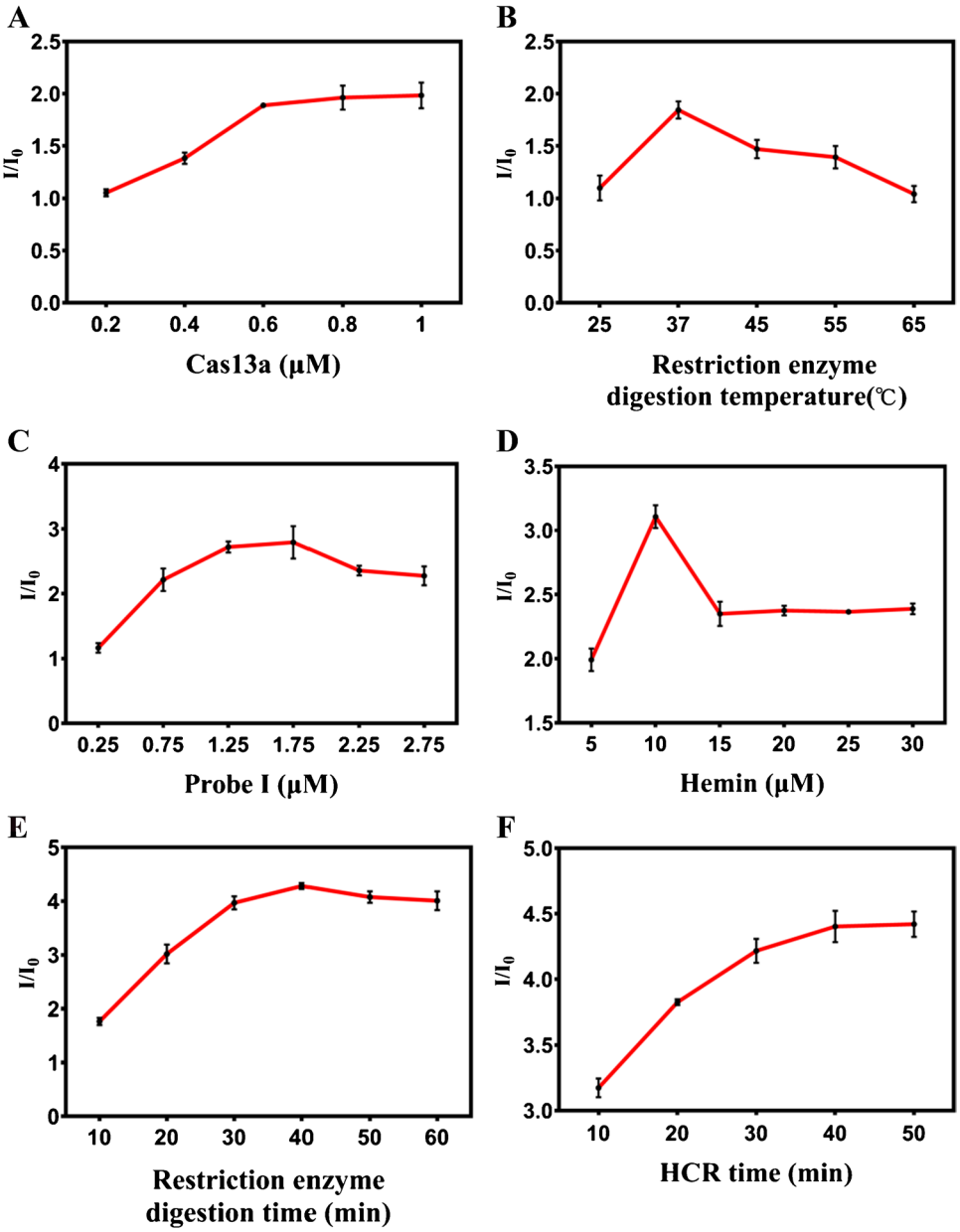

Fig. 2 Optimization of experimental conditions. **A** Cas13a protein concentration. **B** Restriction enzyme digestion temperature. **C** Probe I concentration. **D** Hemin concentration. **E** Restriction enzyme digestion time. **F** HCR time

1.25 μM, there was only a small and negligible increase in absorbance. Considering the cost, 1.25 μM was selected as the optimum amount of primer probe I added. The effect of the concentration between hemin and G-quadruplex was also monitored. The I/I_0 value initially increased and then decreased (Fig. 2D). The I/I_0 value reached a maximum when the concentration of hemin was 10 μM. The concentration was selected as the optimum concentration of hemin. The I/I_0 value increased as the Cas13a/crRNA trans-cleavage time increased from 10 to 40 min (Fig. 2E). When the trans-cleavage time reached 30 min, further increases in time led to a smooth increase in I/I_0 followed by a slight decrease. Thirty minutes was identified as the best digestion time. The I/I_0 value increased with increasing HCR time and reached a peak at 40 min (Fig. 2F). Forty minutes was sufficient for HCR to fully react and was chosen.

The concentration ratio of Na^+ and K^+, and of hairpin H1 and H2, was also optimized. Formation and stabilization of G-quadruplexes depended on cations. In the presence of monovalent cations such as Na^+, K^+, NH_4^+, Rb^+, and others, guanylate-rich DNA or RNA could form a stable G-quadruplex structure. Of these cations, K^+ and Na^+ are ubiquitous in cells, so the concentration ratio of Na^+ and K^+ in the buffer was optimized. When the concentration ratio of Na^+ to K^+ was 1:10, the absorbance value of the sample was the highest (see Supplementary information Figure S2A). The amount of G-quadruplex that formed was closely related to hairpin H1 and H2. Therefore, the concentration ratio of these

hairpins was optimized. The absorbance value increased with increasing concentration ratio. When the concentration ratio of hairpin H1 and H2 reached 2:1.5, the absorbance value was highest. Further increases of the hairpin H2 concentration produced significantly decreased absorbance (see Supplementary information Figure S2B). Therefore, the 2:1.5 concentration ratio of hairpin H1 to H2 was chosen as the optimal condition for the experiment.

Sensitivity

The linear range and sensitivity of the developed sensing system for influenza H1N1 detection were measured using the optimized experimental conditions. The susceptive response relationships between the concentration of the influenza H1N1 target RNA probe and the variance of absorption intensity indicated variable absorption intensity with increasing concentration of target RNA extracted from influenza H1N1 (10^1, 10^2, 10^3, 10^4, and 10^5 pM) (Fig. 3A). Over the range of $10^1 \sim 10^5$ pM, good linear correlation from signal change and lg (target RNA concentration) was observed (Fig. 3B). The regression equation was $I/I_0 = 1.057 \log_{10}C - 0.1560$ ($R^2 = 0.912$). The limit of detection was calculated as 0.152 pM based on 3σ/slope, where σ is the standard deviation and k represents the slope of the line. Compared with several CRISPR/Cas detection systems, in terms of time and sensitivity, our detection method was comparable or superior (see Supplementary information Table S2).

Specificity

An excellent virus method has the ability to distinguish influenza viruses based on their subtype and high similarity sequence. The specificity of the colorimetric biosensor was evaluated by four influenza viruses (H3N2, H5N1, H9N2, and H7N9) and other three types of probes for base mutation (M1, M2, and M3 represent one base mutation, two base mutations, and three base mutations, respectively). As shown in Fig. 4, at the same concentration (100 nM), the altered signal intensity about influenza viruses in the same system and similar sequences did not obviously differ from that of the background (no addition of target RNA); only H1N1 RNA produced a prominent altered signal. These results indicated that the detection method has good specificity, with good resolution of even a single base mutation.

Analysis of spiked serum samples

Influenza H1N1 virus can be detected in serum following infection. To assess the practical feasibility of the developed method, different concentrations of H1N1 target RNA probe (1, 10, and 100 nM) were added to 10 × diluted serum. The H1N1 assay was then performed. The recovery for the 1, 10, and 100 nM concentrations of H1N1 target RNA probe was 83.90%, 104.50%, and 104.77%, respectively. The relative standard deviation ranged from 0.27 to 6.95% (Table 1). These findings suggested the potential value and practicability of this colorimetric biosensor to monitor influenza H1N1 in spiked biological samples.

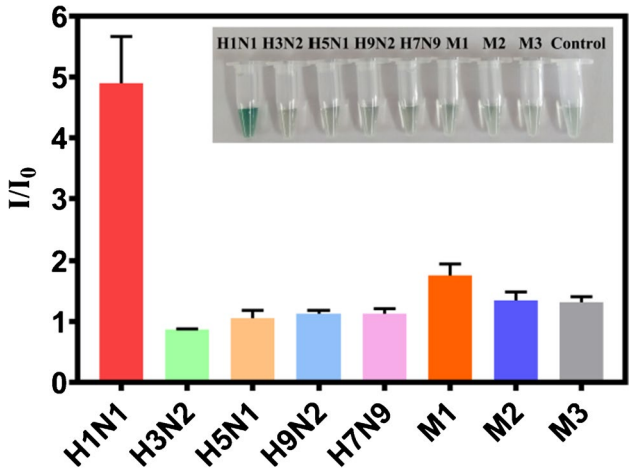

Fig. 4 Selectivity of the proposed method using different influenza virus RNA targets and different probes for base mutation. The concentration of each target RNA was 100 nM, and the other conditions remained the same

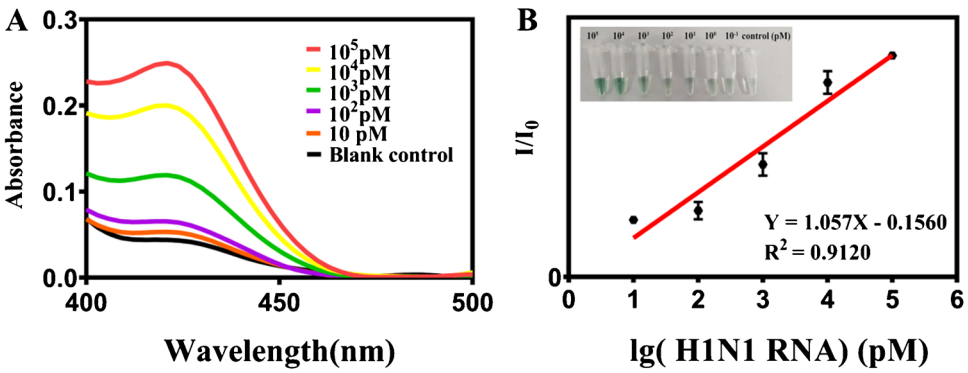

Fig. 3 **A** Concentration of H1N1 target RNA from 100 nM to 10 pM, and the intensity of colorimetric change. **B** Analysis of the linear relationship between the concentration of H1N1 target RNA (100 nM ~ 10 pM) and the intensity of colorimetric change

Table 1 Recovery test of H1N1 target RNA detection in tenfold diluted serum samples ($n=3$)

Samples	Added (nM)	Found (nM)	Recovery (%)	RSD (%)
1	100	104.77	104.77	0.27
2	10	10.45	104.50	2.71
3	1	0.839	83.90	6.95

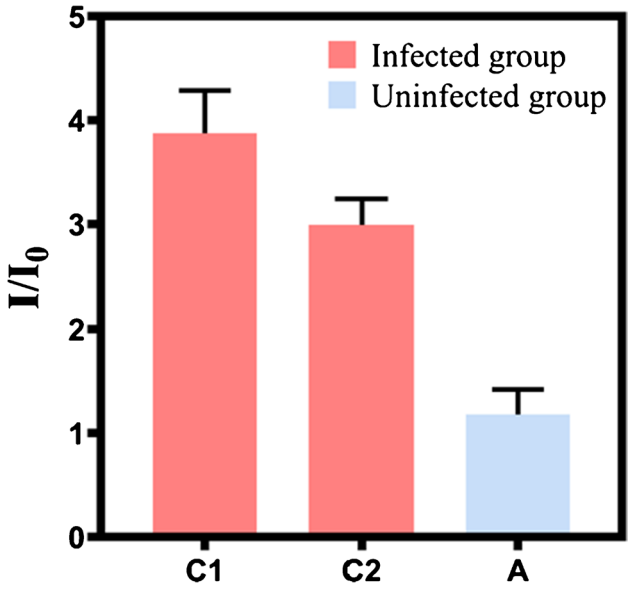

Fig. 5 Absorbance values of infected and uninfected groups. C represents the infected group and A represents the uninfected group. H1N1 influenza virus titer (C1: 1.0×10^8 copies/mL, C2: 1.0×10^7 copies/mL) in allantoic fluid samples

Real-sample analysis

We further examined the applicability and specificity of the colorimetric biosensor in detecting target RNA in complicated RNA extracts. To verify the accuracy of this sensing method, the colorimetric biosensor was used to detect influenza H1N1 in allantoic fluid of chicken embryo samples. The total RNA of the virus at this concentration was extracted from 1.0×10^8 copies/mL virus titer, according to this experimental method. As shown in Fig. 5, the results of the experimental group (infected group) and the control group (uninfected group) were significantly different. This result demonstrates that this experimental approach could accurately capture target RNAs in complex RNA samples. Therefore, the assay presented in this experiment is a promising tool for the detection of H1N1 influenza virus in complex matrices.

Conclusions

We describe the establishment and verification of a CRISPR/Cas13a-based visual influenza H1N1 viruses label-free and isothermal detection method. An oligonucleotide probe I strand was designed as a trans-cleavage substrate for Cas13a/crRNA and was used as a primer for HCR after cleavage. Our method adopts a dual signal amplification strategy, which can greatly increase sensitivity. The novel detection method has a detection limit of 0.152 pM for influenza H1N1 with excellent linearity between 10 pM and 100 nM. The assay also has excellent specificity. Other influenza A viruses and highly homologous RNA probes with only a single base difference can be clearly distinguished. The method does not require a variable-temperature environment and special expensive equipment, and is fast and efficient. The novel method could be valuable for biological research and clinical detection of virus.

Supplementary Information The online version contains supplementary material available at https://doi.org/10.1007/s00216-022-04380-1.

Acknowledgements This work was financially supported by the Science and Technology Development Plans of Jilin Province (20150101105JC).

Declarations

Conflict of interest The authors declare no competing interests.

References

1. Sandrock C, Kelly T. Clinical review: update of avian influenza A infections in humans. Crit Care. 2007;11(2):209. https://doi.org/10.1186/cc5675.
2. Taubenberger JK, Morens DM. 1918 influenza: the mother of all pandemics. Emerg Infect Dis. 2006;12(1):15–22. https://doi.org/10.3201/eid1201.050979.
3. Hay AJ, Gregory V, Douglas AR, Lin YP. The evolution of human influenza viruses. Philos Trans R Soc Lond B Biol Sci. 2001;356(1416):1861–70. https://doi.org/10.1098/rstb.2001.0999.
4. Molini U, Curini V, Jacobs E, Tongo E, Berjaoui S, Hemberger MY, et al. First influenza D virus full-genome sequence retrieved from livestock in Namibia. Africa Acta Trop. 2022;232: 106482. https://doi.org/10.1016/j.actatropica.2022.106482.
5. Cheng VC, To KK, Tse H, Hung IF, Yuen KY. Two years after pandemic influenza A/2009/H1N1: what have we learned? Clin Microbiol Rev. 2012;25(2):223–63. https://doi.org/10.1128/CMR.05012-11.
6. Medina RA, Garcia-Sastre A. Influenza A viruses: new research developments. Nat Rev Microbiol. 2011;9(8):590–603. https://doi.org/10.1038/nrmicro2613.
7. Merckx J, Wali R, Schiller I, Caya C, Gore GC, Chartrand C, et al. Diagnostic accuracy of novel and traditional rapid tests for influenza infection compared with reverse transcriptase polymerase chain reaction: a systematic review and meta-analysis. Ann Intern Med. 2017;167(6):394–409. https://doi.org/10.7326/M17-0848.
8. Ji Y, Guo W, Zhao L, Li H, Lu G, Wang Z, et al. Development of an antigen-capture ELISA for the detection of equine influenza virus nucleoprotein. J Virol Methods. 2011;175(1):120–4. https://doi.org/10.1016/j.jviromet.2011.04.016.
9. Cong Y, Sun Y, Deng X, Yu H, Lian X, Cong Y. A SYBR green-based real-time RT-PCR assay to differentiate the H1N1 influenza virus lineages. J Virol Methods. 2022;300: 114387. https://doi.org/10.1016/j.jviromet.2021.114387.
10. Kim SO, Kim SS. Bacterial pathogen detection by conventional culture-based and recent alternative (polymerase chain reaction, isothermal amplification, enzyme linked immunosorbent assay, bacteriophage amplification, and gold nanoparticle aggregation)

methods in food samples: a review. J Food Saf. 2021;41(1): e12870. https://doi.org/10.1111/jfs.12870.
11. Tepeli Y, Anik U. Electrochemical biosensors for influenza virus a detection: the potential of adaptation of these devices to POC systems. Sensor Actuat B-Chem. 2018;254:377–84. https://doi.org/10.1016/j.snb.2017.07.126.
12. Chen H, Park SG, Choi N, Moon JI, Dang HJ, Das A, et al. SERS imaging-based aptasensor for ultrasensitive and reproducible detection of influenza virus A. Biosens Bioelectron. 2020;167: 112496. https://doi.org/10.1016/j.bios.2020.112496.
13. Nguyen AVT, Dao TD, Trinh TTT, Choi DY, Yu ST, Park H, et al. Sensitive detection of influenza a virus based on a CdSe/CdS/ZnS quantum dot-linked rapid fluorescent immunochromatographic test. Biosensors & bioelectronics. 2020;155. https://doi.org/10.1016/j.bios.2020.112090.
14. Raji MA, Aloraij Y, Alhamlan F, Suaifan G, Weber K, Cialla-May D, et al. Development of rapid colorimetric assay for the detection of influenza A and B viruses. Talanta. 2021;221: 112090. https://doi.org/10.1016/j.talanta.2020.121468.
15. Oshiro S, Tabe Y, Funatogawa K, Saito K, Tada T, Mizutani N, et al. Assessment of an immunochromatographic kit for detection of severe acute respiratory syndrome coronavirus 2 and influenza viruses. J Virol Methods. 2022;302: 114477. https://doi.org/10.1016/j.jviromet.2022.114477.
16. Ma YD, Chen YS, Lee GB. An integrated self-driven microfluidic device for rapid detection of the influenza A (H1N1) virus by reverse transcription loop-mediated isothermal amplification. Sensor Actuat B-Chem. 2019;296: 126647. https://doi.org/10.1016/j.snb.2019.126647.
17. Makarova KS, Wolf YI, Alkhnbashi OS, Costa F, Shah SA, Saunders SJ, et al. An updated evolutionary classification of CRISPR-Cas systems. Nat Rev Microbiol. 2015;13(11):722–36. https://doi.org/10.1038/nrmicro3569.
18. Abudayyeh OO, Gootenberg JS, Konermann S, Joung J, Slaymaker IM, Cox DBT, et al. C2c2 is a single-component programmable RNA-guided RNA-targeting CRISPR effector. Sci (New York, NY). 2016;353(6299):aaf5573. https://doi.org/10.1126/science.aaf5573.
19. Kaminski MM, Alcantar MA, Lape IT, Greensmith R, Huske AC, Valeri JA, et al. A CRISPR-based assay for the detection of opportunistic infections post-transplantation and for the monitoring of transplant rejection. Nature Biomedical Engineering. 2020;4(6):601–9. https://doi.org/10.1038/s41551-020-0546-5.
20. Chen PR, Wang LY, Qin PP, Yin BC, Ye BC. An RNA-based catalytic hairpin assembly circuit coupled with CRISPR-Cas12a for one-step detection of microRNAs. Biosens Bioelectron. 2022;207: 114152. https://doi.org/10.1016/j.bios.2022.114152.
21. Abudayyeh OO, Gootenberg JS, Essletzbichler P, Han S, Joung J, Belanto JJ, et al. RNA targeting with CRISPR-Cas13. Nature. 2017;550(7675):280. https://doi.org/10.1038/nature24049.
22. Koonin EV, Makarova KS, Zhang F. Diversity, classification and evolution of CRISPR-Cas systems. Curr Opin Microbiol. 2017;37:67–78. https://doi.org/10.1016/j.mib.2017.05.008.
23. Huang MQ, Huang R, Yue HH, Shan YY, Xing D. Ultrasensitive and high-specific microRNA detection using hyper-branching rolling circle amplified CRISPR/Cas13a biosensor. Sensor Actuat B-Chem. 2020;325: 128799. https://doi.org/10.1016/j.snb.2020.128799.
24. Wang YX, Xue T, Wang MJ, Ledesma-Amaro R, Lu Y, Hu XY, et al. CRISPR-Cas13a cascade-based viral RNA assay for detecting SARS-CoV-2 and its mutations in clinical samples. Sensor Actuat B-Chem. 2022;362: 131765. https://doi.org/10.1016/j.snb.2022.131765.
25. Zhao J, Li B, Ma J, Jin W, Ma X. Photoactivatable RNA N(6) -methyladenosine editing with CRISPR-Cas13. Small. 2020;16(30): e1907301. https://doi.org/10.1002/smll.201907301.
26. Zhou T, Huang M, Lin J, Huang R, Xing D. High-fidelity CRISPR/Cas13a trans-cleavage-triggered rolling circle amplified DNAzyme for visual profiling of microRNA. Anal Chem. 2021;93(4):2038–44. https://doi.org/10.1021/acs.analchem.0c03708.
27. Chang Y, Deng Y, Li T, Wang J, Wang T, Tan F, et al. Visual detection of porcine reproductive and respiratory syndrome virus using CRISPR-Cas13a. Transbound Emerg Dis. 2020;67(2):564–71. https://doi.org/10.1111/tbed.13368.
28. Song P, Zhang P, Qin K, Su F, Gao K, Liu X, et al. CRISPR/Cas13a induced exponential amplification for highly sensitive and specific detection of circular RNA. Talanta. 2022;246: 123521. https://doi.org/10.1016/j.talanta.2022.123521.
29. Zhang DY, Seelig G. Dynamic DNA nanotechnology using strand-displacement reactions. Nat Chem. 2011;3(2):103–13. https://doi.org/10.1038/nchem.957.
30. Dirks RM, Pierce NA. Triggered amplification by hybridization chain reaction. Proc Natl Acad Sci USA. 2004;101(43):15275–8. https://doi.org/10.1073/pnas.0407024101.
31. Wu J, Lv J, Zheng X, Wu ZS. Hybridization chain reaction and its applications in biosensing. Talanta. 2021;234: 122637. https://doi.org/10.1016/j.talanta.2021.122637.
32. Travascio P, Li Y, Sen D. DNA-enhanced peroxidase activity of a DNA-aptamer-hemin complex. Chem Biol. 1998;5(9):505–17. https://doi.org/10.1016/s1074-5521(98)90006-0.
33. Travascio P, Witting PK, Mauk AG, Sen D. The peroxidase activity of a hemin–DNA oligonucleotide complex: free radical damage to specific guanine bases of the DNA. J Am Chem Soc. 2001;123(7):1337–48. https://doi.org/10.1021/ja0023534.